Chapter 26

Flying Robots

Stefan Leutenegger, Christoph Huerzeler, Amanda K. Stowers, Kostas Alexis, Markus Achtelik, David Lentink, Paul Oh and Roland Siegwart

Unmanned Aircraft Systems (UAS) have drawn increasing attention recently, owing to advancements in related research, technology and applications. While having been deployed successfully in military scenarios for decades, civil use cases have lately been tackled by the robotics research community.

This chapter overviews the core elements of this highly interdisciplinary field; the reader is guided through the design process of aerial robots for various applications starting with a qualitative characterization of different types of UAS. Design and modeling are closely related, forming a typically iterative process of drafting and analyzing the related properties. Therefore, we overview aerodynamics and dynamics, as well as their application to fixed-wing, rotary-wing, and flapping-wing UAS, including related analytical tools and practical guidelines. Respecting use-case specific requirements and core autonomous robot demands, we finally provide guidelines to related system integration challenges.

be assessed depending on the parameters of the UAV configuration under investigation. Such parameters may for example include the body pitch and roll inertia, the location of the body center of gravity or the location of the rotors or propellers. The fundamental understanding gained in this evaluation process is crucial for the development of effective robotic flight systems and the required control laws.

26.6 Flapping Wing Modeling and Design

A variety of animals, from insects to birds, are capable of flight maneuvers which are presently impossible in micro aerial vehicles, such as flying in turbulence or cluttered airspace. Additionally, animals are more maneuverable and can fly longer distances. People have made many attempts at building flapping robots or ornithopters. While several are successful, many either never take off or fly only for a short duration due to their higher complexity or poor design. Until recently, ornithopters represented a niche of flying vehicles. The development of lithium polymer batteries produced a light-weight high-power energy resource to power ornithopters. Amongst the first successful electric ornithopters were the Caltech & Aerovironment microbats in 1998 [60, 61]. Many designs still fail to fly despite the rapidly increasing population building electric ornithopters. A major problem in most designs is an inability to generate enough lift to take off in the first place. This precludes additional flight research, such as maneuverability, flight distance or time. Engineers have believed that flapping wings are essential to further development of micro aerial vehicles since the first electric ornithopters took off and biologists started to understand the aerodynamics of flapping insect wings. The main reason behind this focus is the idea that they are aerodynamically more efficient at the small Reynolds number of insects (10-10,000) when viscosity effects start to dominate airflow.

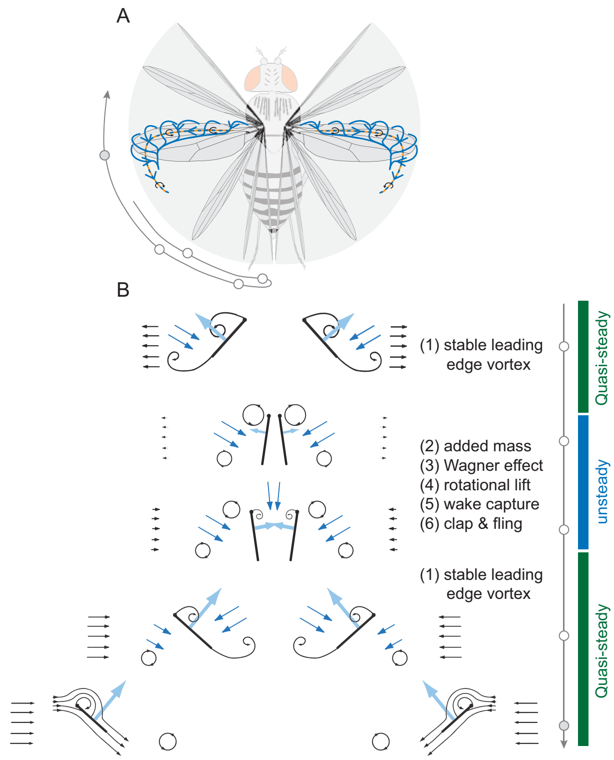

Figure 26.31: Flapping insect wing aerodynamics can be understood through the interaction of a myriad of complex aerodynamic mechanisms. (A) The key high-lift mechanism insects employ, is a stable leading edge vortex (LEV) generated during the up and downstroke. (B) A flapping cycle consists of a quasi-steady part during which the wing accelerates little. During this phase, the stable LEV is the key high-lift mechanism (1). During stroke reversal there is evidence that up to five effects ((2)-(6)) could be important [After Sane [66]].

26.6.1 Aerodynamic Mechanisms

Our understanding of insect aerodynamics provides us with the most detailed model of the aerodynamic function of a flapping wing [18]. There is some evidence that wing flexibility can improve aerodynamic performance of a flapping wing by roughly 10% [77] if the angle of attack is not optimized for a stiff wing. However, a parametric study using a robot model of an insect wing suggests that wing flexibility does not improve performance if we can optimize angle of attack independently of wing stiffness [80]. Ignoring aeroelastic effects that change angle of attack distribution, the key known aerodynamic mechanisms of a flapping wing are [18]:

1. A stable leading edge vortex (LEV) that enables the wing to operate at high angles of attack without stall during the quasi-steady mid-stroke phase (Figure 26.31). During stroke reversal the aerodynamics is not quasi-steady. In this phase, five additional affects are thought to be important:

2. "Added mass" effects due to fluid acceleration in response to the reversal.

3. The Wagner effect explaining that changes in vortex strength need time to build-up over a few chord lengths of travel.

4. Rotational lift due to the timing of changes in angle of attack during stroke reversal and its effect on vortex lift through the "Kramer effect".

5. Wake capture when the wing reverses direction and interacts with the momentum jet of its shed wake.

6. Clap and fling when the wings become close enough to (nearly) touch and air is forced out of the cavity formed by the two wings and sucked back in, which can increase lift [38].

There exist, however no quantitative experimental studies or theories that fully dissect these effects and quantify their relative importance for aerodynamic lift and power. Whereas flapping wing aerodynamics is complex and not fully understood, it is simple from a robot design perspective, because it is scalable from insect to bird size (Figure 26.32). This enables prototyping at larger, more cost effective, scales and enables scaling the design down as technology advances, and smaller components and fabrication methods become available [41]. Flapping wings generate more lift than translating wings because they generate a stable LEV. To generate a stable vortex over the whole wing, the aspect ratio with respect to the center of rotation needs to be equal to or smaller than about 4 [40]. Flapping wings with an aspect ratio larger than 4 can stall outboard [40]; whereas more stubby flapping wings cannot. This can explain why the majority of insect, bird and bat wings have an aspect ratio of around 2-4 with respect to the "shoulder" joint [40]. The main advantage of stubby wings is that they do not stall at high angles of attack enabling animals to take-off and land vertically by increasing angle of attack instead of flapping frequency [40] using LEVs [69]. Insects [21], bats, hummingbirds [74], and other birds [51], but also auto rotating seeds generate stable LEVs. This shows that stable LEVs are a convergent evolutionary solution for high lift at high angle of attack in nature [40].

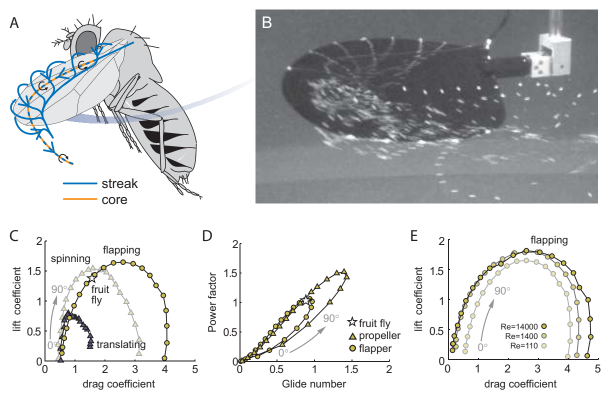

Figure 26.32: The aerodynamics of a flapping (insect) wing scale from insect to bird scale. (A) A stable LEV enables flapping wings to operate at high angles of attack without stall. (B) The key parameter explaining LEV stability is the wing's swing, its spinning motion, as demonstrated by this spinning model of a fly wing which generates a stable LEV and similarly elevated forces as in flapping wings. (C) At insect scale fixed (translating) wings underperform, whereas flapping and spinning wings generate similarly high lift. Spinning wings generate less drag which makes them more efficient. (D) The power factor of a spinning wing is higher than for a flapping wing, higher indicating that less power is needed to support body weight. (E) The dimensionless lift and drag averaged over a full flapping cycle is independent of scale to within good approximation (Reynolds number 110: fruit fly; 1,400; house fly; 14,000; hummingbird). This makes flapping wing aerodynamics scalable enabling the use of dimensional analysis [41].

Comparison of flapping versus spinning (propeller-like) insect wings shows spinning insect wings generate similar elevated lift forces by generating a LEV at lower drag. Helicopters with stubby rotors are, therefore, aerodynamically more efficient than stubby flapping wings, because they need less power to fly, as qualitatively presented in Figure 26.32D [41]. This is confirmed experimentally for the most advanced hovering ornithopter at present, the Nano Hummingbird [32]. Comparing its flapping wing with a spinning wing showed for various forward speeds that flapping wings require more power for the same lift, in part due to aerodynamics [41, 40], and in part due to inertia losses [41, 32]. The key advantage of flapping wings seems to be the potential for extreme maneuverability and robustness. For instance flapping wings may fare better in turbulence, close to the ground, near vertical surfaces and through clutter, when helicopters can become unstable due to stall and complex rotor-wake interactions [34].

26.6.2 Sizing New Flappers

An improved understanding of the detailed aerodynamics is scientifically invaluable, but perhaps not critical for designing successful ornithopters at a time when most struggle to take-off. Instead, sizing an ornithopter in terms of gross design parameters such as wing span, weight, and flapping frequency is more critical for take-off. The design methodology introduced here explains how one can transform successful designs to meet other mission perspectives. These designs can then enable flight studies that can advance our understanding of ornithopters versus RoUAS and FW-UAS to better appreciate their unique advantages.

Amongst successful flappers, there are three main archetypes as shown in Figure 26.33. Historically, most flappers have relied on variants of a 4-bar mechanism to generate the flapping motion which generates lift. One example of this is the DelFly family of ornithopters, which are capable of both fast forward flying and hover using this approach. A recent design which demonstrates both prolonged hovering flight and maneuverability, although lacks the ability to fly fast forward, is the Aerovironment Nano-Hummingbird [32]. The Nano-Hummingbird uses a flapping mechanism composed of rollers and strings, while still using a geared down motor to provide power at the right frequency. Additionally, the wings provide control, rather than traditional tail control surfaces. Another more modern development is centimeter scale ornithopters which use piezoelectric actuators to generate flapping motion and control such as the Harvard Fly [45] and the Berkeley Micromechanical Flying Insect. These are capable of tethered flight only, because no batteries exist that can supply high enough power in a lightweight enough package.

	Delfly II	Nano-Hummingbird	RoboBee
Wingspan (cm)	28	16	3
Mass (g)	16	19	0.06
m/m_0	1.26	1.37	N/A (tethered)
Flight time	15 min.	11 min.	N/A (tethered)
Frequency (Hz)	14	30	110
Mechanism	Gearbox and 4-bar	Gearbox and string rollers	Piezo-electric Elastic 4-bar like
Scale (mm)	10^2-10^0	10^2-10^0	10^2-10^{-1}
Power	1.4 W	3.27 W	N/A (tethered)
Current	380 mA	880 mA	N/A (tethered)

Figure 26.33: Examples of three different types of successful flappers. Photo credits: A: Jaap Oldenkamp, B: [32], C: [45]. Sources: DelFly II [41, 14], Nano Hummingbird [32], RoboBee [45]

Despite the differences in design, these flappers share common trends in parameters, as shown in Figure 26.34. To design a functional ornithopter, we start with a desired mission such as surveillance, search and rescue, or military applications. The mission determines an appropriate wingspan, and also determines a minimum time for task completion. Figure 26.34 shows that empty weight (mass without battery) follows an exponential pattern with wingspan, especially over the mid-range of wingspans. The main observation is that the power defining scale is not 3, but approximately 1.5. This may be because significant portions of the mass of smaller ornithopters comes from electronics, gearboxes and actuators, whose masses are not dependent on wingspan. Additionally, required flapping frequency decreases with wingspan, enabling an approximation of required flapping frequency based on wingspan that works well for all sizes of ornithopters, as expected using scaling relations.

Using initial design parameters from a successful ornithopter, we can design another ornithopter that is also capable of flapping flight using scaling rela-

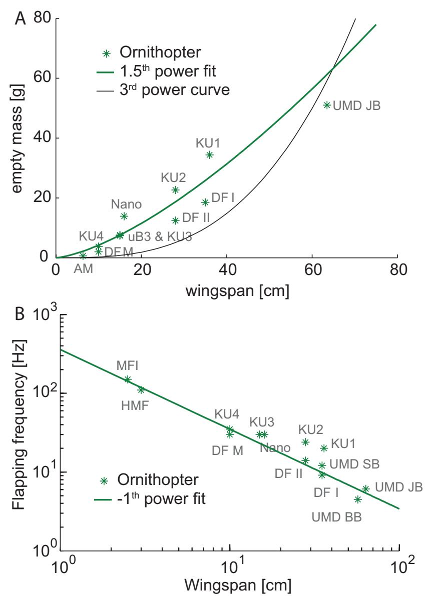

Figure 26.34: Current ornithopter trends of empty mass and flapping frequency with changes in wingspan. (A) The empty mass of successful ornithopters does not scale with wingspan cubed, but with wingspan to the power 1.5 (R^2=0.79). The power law predicts the approximate masses effectively in the 10-50 cm wingspan range, while it overestimates the mass for those with wingspans below 10 cm. The curve to the third power consistently underestimates the unloaded masses of current ornithopters. (B) To support the weight of the ornithopter, flapping frequency needs to increase inverse to wingspan for smaller wingspans. Ornithopters in (A) fly freely and have a flight time of at least one minute. The Micromechanical Flying Insect and Harvard Fly follow the same trend line for flapping frequency as larger ornithopters; even though they fly tethered (they would need to flap faster with batteries onboard). The relationship here fits a power curve with the exponent equal to -1.01 with R^2=0.96. Abbreviations are as follows: MFI-Berkeley Micromechanical Flying Insect; HMF-Harvard Microfly (Robobee); KU1,2,3,4-Konkuk University ornithopters; DFI,II,M-Delfly I,II and Micro; Nano-Aerovironment Nano-Hummingbird; UMD SB, JB, BB-University of Maryland Small Bird, Big Bird, Jumbo Bird; AM-Brian's Ornithopter; uB3-NiCad powered Caltech Microbat

tionships of geometry, fluid mechanics and battery physics [8]. We need to decide on design parameters for the new flapper, including the wingspan b, weight W, aspect ratio Λ, and battery weight W_{batt}. Here, the aspect ratio is wingspan divided by chord length, as these are both easily measured design parameters. Example of initial parameters for the Delfly II are: $b_1 = 28\,\text{cm}$, $m_1 = 16\,\text{g}$ ($W = mg$), $\Lambda_1 = 3.5$, $f_1 = 14\,\text{Hz}$, $P_1 = 1.4\,\text{W}$, $W_{\text{batt},1} = 2.7\,\text{g}$, $t_1 = 15\,\text{min}$. Initial design parameters are denoted with subscript 1; while new design parameters are denoted with subscript 2. Using the curve fitted through successful ornithopters as shown in Figure 26.34, one can make an initial approximation of empty weight. First, we can calculate the wing area, A_{fl}, of the new flapper and the old flapper using the same equation for each:

$$A \propto \frac{b^2}{\Lambda}. \tag{26.94}$$

In hovering or steady forward flight, it is reasonable to assume that weight is proportional to lift:

$$W \propto \frac{1}{2} c_L \rho V_t^2 A_{\text{fl}}. \tag{26.95}$$

We assume that c_L (lift coefficient), ρ (density) and g (gravitational acceleration) are constant [41], which is reasonable for flights on earth at low altitudes. Then, rearranging produces the following relationship between forward velocities, V_t:

$$V_{t,2} = V_{t,1} \sqrt{\frac{W_2}{W_1} \frac{A_{\text{fl},1}}{A_{\text{fl},2}}}. \tag{26.96}$$

We can then assume that the advance ratio, J, is constant for both vehicles, which is a reasonable approximation for ornithopters with similar wing kinematics, shape, and deformation. The advance ratio, J, is the ratio of maximum forward speed to wingtip speed:

$$J = \frac{V_t}{4 f \Phi R}. \tag{26.97}$$

Since wingspan is twice the radius, and we can use the assumption that J is constant to obtain the following relationship for flapping frequencies:

$$f_2 = \frac{V_{t,2}}{V_{t,1}} \frac{b_1}{b_2} \frac{\Phi_1}{\Phi_2} f_1. \tag{26.98}$$

Then, assuming that flapping amplitude, Φ is constant between the two designs (reasonable for designs that follow the same parameters and keep the same gearboxes) we can simplify the relationship for flapping frequencies:

$$f_2 = \frac{V_{t,2}}{V_{t,1}} \frac{b_1}{b_2} f_1. \tag{26.99}$$

The required power to fly is proportional to the weight and flight speed:

$$P \propto mgV_t = WV_t. \tag{26.100}$$

Thus we can calculate the power required of the new flapper relative to that of the old flapper:

$$P_2 = P_1 \frac{V_{t,2}}{V_{t,1}} \frac{W_2}{W_1}. \tag{26.101}$$

Using the power calculated above, the flight time can be estimated as

$$t = \frac{C_{\text{LiPo}} U_{\text{LiPo}}}{P} m, \tag{26.102}$$

in which U_{LiPo}=3.7 V for a LiPo battery, and where, as in 26.35, the capacity can be approximated as:

$$C_{\text{LiPo}} = m_{\text{batt}} k_{\text{batt}}. \tag{26.103}$$

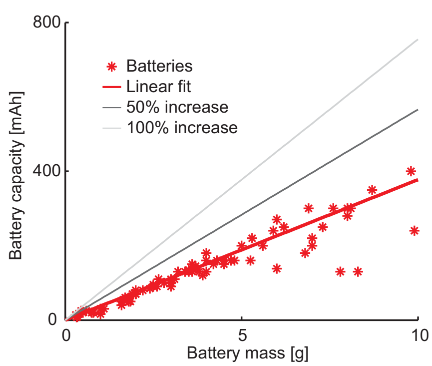

Figure 26.35: Battery capacity as a function of mass for many small lithium polymer (LiPo) batteries in the size range (<10g) which would be used for ornithopters with 10-50cm wingspan. The graph shows the technology is linearly scalable. The approximate capacity density of small LiPo cells (3.7 V) is 37 mAh/g.

From the scaling equations (particularly (26.101) and (26.102)), we can produce a set of graphs as in Figure 26.36, allowing us to use the wingspan and flight time to design a scaled ornithopter. Beginning with the approximate wingspan and flight time desired, we use Figure 26.36A to choose the appropriate battery mass. An increase in wingspan creates the option for heavier batteries and an increase in flight time as does an increase in battery mass. The wingspan and battery mass specify the required flapping frequency. This allows us to choose a motor

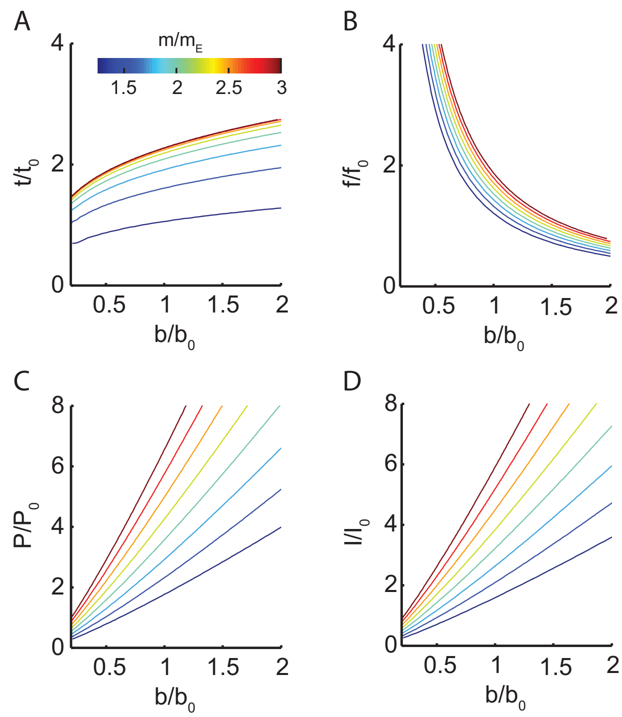

Figure 26.36: These four figures show the effects of changing wingspan and adding battery mass to an ornithopter on the flight time, power consumption, current requirement, and flapping frequency requirement. The value of the empty mass, m_e, is determined using the fitted curve in Figure 26.34A for each wingspan. The figures are then scaled from the initial reference (Delfly II) whose position is at (1,1) in each figure. (A) Increasing the battery mass ratio increases the flight time up until the ratio becomes equal to 3. This ignores additional airframe mass needed to carry these batteries. (B) However, increasing the battery mass also increases the required flapping frequency. (C, D) Increasing the frequency also increases the necessary power and current. Using these parameters, we can iterate back and forth between the plots until a feasible design is found.

and gear ratio. If this turns out to be impractical with available components, we can adjust parameters and iterate between the equations shown in Figure 26.36. In general, for an ornithopter with equal mass, increasing the wingspan decreases the necessary flapping frequency. Alternatively, increasing the battery mass to improve flight time also requires increasing flapping frequency, electric power and current to carry the extra payload. This explains why increasing battery mass beyond empty weight causes little increase in flight time, because the airframe needs to become much stronger at the cost of weight. A penalty in the flight time scaling equation needs to be implemented to correct for the increase in structural weight. The required flapping frequency and battery mass ratio specify the required power. Power increases significantly with wingspan. Additionally, power increases with added battery mass due to the increase in flapping frequency required to lift the larger mass. Finally, we can determine the current the battery needs to supply, which is proportional to the power assuming we use the same kind of battery and efficiency of motor. Iterating between these steps enables finding solutions that best meet the mission specifications. We note that many ornithopters could fly significantly longer by doubling their current battery mass (see Figure 26.36A) at the expense of control response (inertia) and airframe loading.

If flight time needs to increase for a wingspan-constrained ornithopter design, and battery mass and chemistry is already optimized, we should reduce airframe mass (see Figure 26.37) and increase wing area [41]. Mass can be further decreased by airframe optimization using underutilized aerospace optimization strategies, and by critically reevaluating the payload. Wing area can be increased by decreasing aspect ratio and selecting a biplane instead of a monoplane configuration. Whereas such wing design changes reduce aerodynamic efficiency of the wing, they increase the overall vehicle energy efficiency, and therefore increase flight time. Ornithopters that fly long enough to complete missions are often controlled by low-weight underpowered actuators that sacrifice maneuverability.

To control the ornithopter's flight and to utilize its maneuverability we need to generate enough control torques with lightweight actuators. Designs optimized for flight time, such as the DelFly, use control surfaces added to the tail in the style of a traditional rudder or elevator. More maneuverable designs use the flapping wings as control surfaces, by changing their angle of attack (Nano-Hummingbird [32]) or left

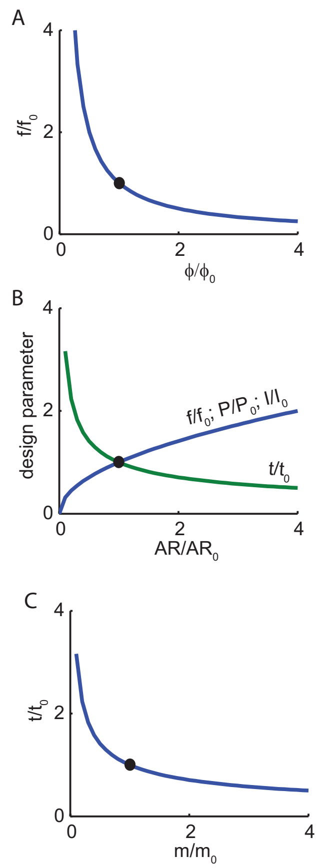

Figure 26.37: Changing additional parameters can modify performance of a scaled vehicle. (A) Adjusting the flapping amplitude allows the user to change the required flapping frequency to use available motor/gearbox combinations. Generally, larger flapping angles result in increased lift coefficient and decreased drag [67]. Thus increasing the amplitude to match it with the motor and gear train can decrease the required power to fly. (B) As the aspect ratio increases at a constant wingspan, the wing area decreases, and therefore the flight time decreases while the required flapping frequency (and hence the power and current) increases. (C) Flight time decreases with additional payload (weight).

versus right wing relative flapping motions (Robobee [45]). The two dominant off the shelf actuators are standard servos and magnetic actuators. Standard servos have small electric motors and potentiometers and move to specified positions; while magnetic actuators have a small magnet inside a small coil of wire and apply specified amounts of torque. Magnetic actuators are available at lower masses than servos, which proves critical in optimizing performance of smaller ornithopters. This shows that selecting appropriate actuators involves a tradeoff between flight duration and maneuverability. Ornithopters that are more maneuverable require more powerful and precise servo actuators. The required servo torque of a scaled ornithopter can be estimated assuming isometric scaling: Torque should be proportional to total weight times wingspan, because aerodynamic force is proportional to weight, and arm length to wingspan. Knowing the required torque, we need to find a servo that can provide it. To reduce trial and error we have plotted current servo data to determine how torque correlates with mass to budget for its weight. The data in Figure 26.38 shows that torque is proportional to mass squared for current servo technology, while empty ornithopter mass scales with wingspan to the power of 1.5 (see Figure 26.34), so as wingspan increases the actuator mass can become proportionally smaller.

We have demonstrated current design strategies based off scaling successful designs that ensure ornithopters fly. These upgraded “rules of thumb” are powerful because current aerospace design analysis and optimization techniques for ornithopters lack predictive power and are therefore less informative than estimates based on scaled flying designs. If current designers base their first iteration of new ornithopters on current state-of-the-art ornithopters, the field can progress at a faster pace through successful flight testing of new concepts that meet novel mission criteria.

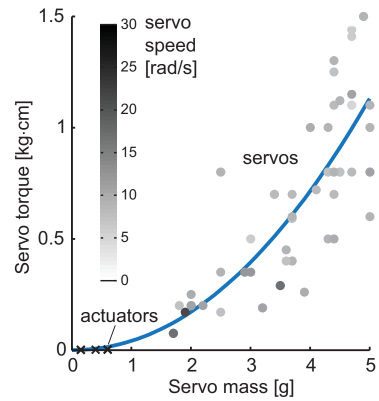

Figure 26.38: Servo (dots) and actuator (crosses) torques increases with mass. The intensity of dots represents the servo speed, with darker dots representing faster servos (the magnetic actuators do not have speeds shown, as they apply a force rather than specify a position). The servo speed does not correlate strongly with mass, as it is dependent on the motors, gears, and other internal hardware of the servo, as well as the supply voltage. There are magnetic actuators available in the range of 0.8-1.8g, they are not included here due to lack of data available from manufacturers.

26.7 System Integration and Realization

Enabling autonomous flights with UAS incorporates solving many challenges. This requires an interdisciplinary approach, bringing together expertise from many different fields. As shown in Figure 26.39, knowledge in the field of aircraft design, as detailed in this chapter, is required, as well as in many fields of engineering and robotics (cf. (REF. APPROPRIATE CHAPTER(S) IN THIS BOOK)).

26.7.1 Challenges for Autonomous UAS

Given the agility of UAS and their strict limitations on weight and power consumption, the choice of sensors, processors and algorithms impose great technical and scientific challenges. Also, major differences exist between ground vehicles and UAS—sensors and algorithms that work well on ground vehicles cannot simply be applied on UAS due to inherent challenges:

Sweden (NEAT) and Wales (Parc Aberporth).

Lastly, somewhat ironic is that today's unmanned drones require a crew of highly–skilled operators. In the case of some Predator missions, crew sizes can be up to a dozen people. Also ironic is that human error is the most cited cause for drone accidents. As the number of UAS in the national airspace increases, the need for even more operators will also grow. This has the potential to raise the risk of UAS–related accidents. The issues of effective UAV pilot training, certifying operators, handling emergency landings, and sharing airports with manned aircraft will also emerge as pressing ones.

26.9 Conclusions and Further Reading

Design of aerial robots requires background knowledge in a multitude of subjects, from aerodynamics to dynamics, control and system integration: we have overviewed the relevant basics along with analytical tools and guidelines to go through the stages of designing, modeling and setting up operation of various types of Unmanned Aerial Systems (UAS). An emphasis was given on costum-tailoring a system to a specific application, in order to optimally meet related requirements in terms of endurance, range, agitlity, size, complexity, as well as from a system integration point of view. The compilation at hand shall serve as a starting point, further motivating the reader to study the various fields with their related literature, ranging from aircraft and system design to the classical autonomous robotics challenges involving perception, cognition and motion control.

Bibliography

[1] Markus W. Achtelik. "Advanced Closed Loop Visual Navigation for Micro Aerial Vehicles". PhD thesis. ETH Zurich, 2014.

[2] Markus W. Achtelik et al. "Motion and Uncertainty Aware Path Planning for Micro Aerial Vehicles". In: *Journal of Field Robotics (JFR)* (2014). Special Issue on Low-Altitude Flight of UAVs.

[3] Michael C Achtelik et al. "Design of a Multi Rotor MAV with regard to Efficiency, Dynamics and Redundancy". In: *AIAA Guidance, Navigation, and Control Conference*. 2012.

[4] A. Bachrach et al. "Estimation, planning, and mapping for autonomous flight using an RGB-D camera in GPS-denied environments". In: *International Journal of Robotics Research (IJRR)* 31.11 (Sept. 2012), pp. 1320–1343. ISSN: 0278-3649.

[5] A Bachrach et al. "RANGE - Robust Autonomous Navigation in GPS-denied Environments". In: *Journal of Field Robotics (JFR)* 28.5 (Sept. 2011), pp. 644–666.

[6] R.W. Beard and T.W. McLain. *Small Unmanned Aircraft: Theory and Practice*. Princeton University Press, 2012. ISBN: 9780691149219.

[7] Samir Bouabdallah. "Design and Control of quadrotors with application to autonomous flying". PhD thesis. Lausanee: STI School of Engineering, EPFL, 2007.

[8] Samir Bouabdallah et al. "Towards Palm–Size Autonomous Helicopters". In: *Proceedings of the International Conference and Exhibition on Unmanned Aerial Vehicles*. 2010.

[9] A.R.S. Bramwell, George Done, and David Balmford. *Bramwell's Helicopter Dynamics*. Butterworth-Heinemann, 2001.

[10] Adam Bry and Nicholas Roy. "Rapidly-exploring Random Belief Trees for motion planning under uncertainty". In: *Proceedings of the IEEE International Conference on Robotics and Automation (ICRA)* 21.Icra (2011), pp. 723–730.

[11] Robert T. N. Chen. *A Survey of Nonuniform Inflow Models of Rotorcraft Flight Dynamics and Control Applications*. Tech. rep. National Aeronautics and Space Administration, 1989.

[12] Robert T. N. Chen. *Effects of Primary Rotor Parameters on Flapping Dynamics*. Tech. rep. National Aeronautics and Space Administration, 1980.

[13] H. Cover et al. "Sparse Tangential Network (SPARTAN): Motion Planning for Micro Aerial Vehicles". In: *Proceedings of the IEEE International Conference on Robotics and Automation (ICRA)*. 2013.

[14] G.C.H.E. de Croon et al. "Design, aerodynamics, and autonomy of the DelFly". In: *Bioinspiration and Biomimetics* (2012).

[15] Rita Cunha. "Advanced Motion Control for Autonomous Air Vehicles". PhD thesis. Instituto Superior Tecnico, Universidade Tecnica de Lisboa, Portugal, 2007.

[16] Cyberhawk: Aerial Inspection and Suervying Specialists. *http://www.thecyberhawk.com/*.

[17] G. Darivianakis et al. "Hybrid Predictive Control for Aerial Robotic Physical Interaction towards Inspection Operations". In: *2014 International Conference on Robotics and Automation (ICRA)*. accepted. Hong Kong, China, 2014.

[18] M.H. Dickinson, F.O. Lehmann, and S.P. Sane. "Wing Rotation and the Aerodynamic Basis of Insect Flight". In: *Science* (1999), pp. 1954–1960.

[19] Patrick Doherty, Jonas Kvarnström, and Fredrik Heintz. "A temporal logic-based planning and execution monitoring framework for unmanned aircraft systems". English. In: *Autonomous Agents and Multi-Agent Systems* 19.3 (2009), pp. 332–377. ISSN: 1387-2532.

[20] G.J.J. Ducard. *Fault-tolerant Flight Control and Guidance Systems: Practical Methods for Small Unmanned Aerial Vehicles*. Advances in Industrial Control. Springer, 2009. ISBN: 9781848825611.

[21] C.P. Ellington et al. "Leading-edge vortices in insect flight". In: *Nature* (1996), pp. 626–630.

[22] B. Etkin. *Dynamics of atmospheric flight*. Wiley, 1972. ISBN: 9780471246206.

[23] Daniel Gurdan et al. "Energy-Efficient Autonomous Four-Rotor Flying Robot Controlled at 1kHz". In: *Proceedings of the IEEE International Conference on Robotics and Autonomous Systems*. 2007.

[24] P.E. Hart, N.J. Nilsson, and B. Raphael. "A Formal Basis for the Heuristic Determination of Minimum Cost Paths". In: *Systems Science and Cybernetics, IEEE Transactions on* 4.2 (1968), pp. 100–107. ISSN: 0536-1567.

[25] Ruijie He, Sam Prentice, and Nicholas Roy. "Planning in Information Space for a Quadrotor Helicopter in a GPS-denied Environments". In: *Proceedings of the IEEE International Conference on Robotics and Automation (ICRA 2008)*. Los Angeles, CA, 2008, pp. 1814–1820.

[26] Gabriel M. Hoffmann et al. "Quadrotor Helicopter Flight Dynamics and Control: Theory and Experiment". In: *Proceedings of the AIAA Guidance, Navigation and Control Conference*. 2007.

[27] E. Raymond Hunt et al. "Acquisition of NIR-Green-Blue Digital Photographs from Unmanned Aircraft for Crop Monitoring". In: *Remote Sensing* 2.1 (2010), pp. 290–305.

[28] ICAO. *Manual of the ICAO Standard Atmosphere: extended to 80 kilometres (262 500 feet)*. ICAO, 1993. ISBN: 9291940046.

[29] K. Alexis, G. Nikolakopoulos and A. Tzes. "Model predictive quadrotor control: attitude, altitude and position experimental studies". In: *Control Theory & Applications, IET* 6.12 (2012), pp. 1812–1827. ISSN: 1751-8644.

[30] Sertac Karaman and Emilio Frazzoli. "Incremental Sampling-based Algorithms for Optimal Motion Planning". In: *Proceedings of Robotics: Science and Systems (RSS)*. Zaragoza, Spain, 2010.

[31] L. E. Kavraki et al. "Probabilistic roadmaps for path planning in high-dimensional configuration spaces". In: *IEEE Transactions on Robotics and Automation* 12.4 (1996), pp. 566–580.

[32] Matthew Keennon et al. "Tailless Flapping Wing Propulsion and Control Development for the Nano Hummingbird Micro Air Vehicle". In: *American Helicopter Society Future Vertical Lift Aircraft Design Conference*. 2012.

[33] Andy Ko, Osgar John Ohnaian, and Paul Gelhausen. "Ducted Fan UAV Modeling and Simulation in Preliminary Design". In: *Proceedings of the AIAA Modeling and Simulation Technologies Conference and Exhibit*. 2007.

[34] J. Koo and T. Oka. *Experimental Study on the Ground Effect of a Model Helicopter Rotor in Hovering*. Tech. rep. NASA, 1966.

[35] AA Lambregts. "Vertical flight path and speed control autopilot design using total energy principles". In: *AIAA paper* 83-2239 (1983).

[36] Steven M. LaValle and James J. Kuffner. "Randomized Kinodynamic Planning". In: *International Journal of Robotics Research (IJRR)* 20.5 (2001), pp. 378–400.

[37] Taeyoung Lee, Melvin Leoky, and N. Harris McClamroch. "Geometric tracking control of a quadrotor UAV on SE(3)". In: *49th IEEE Conference on Decision and Control (CDC)*. IEEE, Dec. 2010, pp. 5420–5425.

[38] F.O. Lehmann, S.P. Sane, and M. Dickinson. "The aerodynamic effects of wing-wing interaction in flapping insect wings". In: *Journal of Experimental Biology* (2005), pp. 3075–3092.

[39] Gordon J. Leishman. *Principles of Helicopter Aerodynamics*. Cambridge University Press, 2006.

[40] D. Lentink and M.H. Dickinson. "Rotational accelerations stabilize leading edge vortices on revolving fly wings". In: *Journal of Experimental Biology* (2009), pp. 2705–2719.

[41] D. Lentink, S.R. Jongerius, and N.L. Bradshaw. *Flying Insects and Robots: The Scalable Design of Flapping Micro Aerial Vehicles Inspired by Insect Flight*. Springer-Verlag, 2009.

[42] Stefan Leutenegger, Margarita Chli, and Roland Yves Siegwart. "BRISK: Binary robust invariant scalable keypoints". In: *Computer Vision (ICCV), 2011 IEEE International Conference on*. IEEE. 2011, pp. 2548–2555.

[43] Stefan Leutenegger et al. "Keyframe-Based Visual-Inertial SLAM Using Nonlinear Optimization". In: *Proceedings of Robotics: Science and Systems (RSS)*. 2013.

[44] Quentin Lindsey, Daniel Mellinger, and Vijay Kumar. "Construction with quadrotor teams". In: *Autonomous Robots* 33.3 (2012), pp. 323–336.

[45] K.Y. Ma et al. "Controlled Flight of a Biologically Inspired, Insect-Scale Robot". In: *Science* (2013), pp. 603–607.

[46] Lorenzo Marconi, Roberto Naldi, and Luca Gentili. "Modelling and control of a flying robot interacting with the environment". In: *Automatica* 47.12 (2011), pp. 2571 –2583. ISSN: 0005-1098.

[47] B.W. McCormick. *Aerodynamics, aeronautics, and flight mechanics*. Wiley, 1979. ISBN: 9780471030324.

[48] Bernard Mettler, Chris Dever, and Eric Feron. "Scaling effects and dynamic characteristics of miniature rotorcraft". In: *Journal of guidance, control, and dynamics* 27.3 (2004), pp. 466–478.

[49] Bernhard Mettler. *Identification, Modeling and Characteristics of Miniature Rotorcraft*. Kluwer Academic Publisher, 2002.

[50] Anastasios I. Mourikis, Stergios I. Roumeliotis, and Joel W. Burdick. "SC-KF Mobile Robot Localization: A Stochastic Cloning Kalman Filter for Processing Relative-State Measurements". In: *IEEE Transactions on Robotics (T-RO)* 23.4 (Aug. 2007), pp. 717–730.

[51] F.T. Muijres, L.C. Johansson, and A. Hedenstrom. “Leading edge vortex in a slow-flying passerine”. In: *Biology Letters* (2012), pp. 554–557.

[52] Roberto Naldi, Francesco Forte, and Lorenzo Marconi. “A Class of Modular Aerial Robots”. In: *Proceedings of the 50th IEEE Conference on Decision and Control and European Control Conference*. 2011.

[53] Janosch Nikolic et al. “A UAV system for inspection of industrial facilities”. In: *Aerospace Conference, 2013 IEEE*. IEEE. 2013, pp. 1–8.

[54] Michael C. Y. Niu. *Airframe Structural Design*. Conmilit Press LTD, 1988. ISBN: 962712804X.

[55] Kenzo Nonami. *Autonomous Flying Robots: Unmanned Aerial Vehicles and Micro Aerial Vehicles*. Springer, 2010.

[56] Andr Noth. “Design of Solar Powered Airplanes for Continuous Flight”. PhD thesis. Autonomous Systems Lab, ETH Zrich, Switzerland, 2008.

[57] Gareth D. Padfield. *Helicopter Flight Dynamics*. Blackwell Publishing, 2007.

[58] Sanghyuk Park, John Deyst, and Jonathan P How. “A new nonlinear guidance logic for trajectory tracking”. In: *AIAA Guidance, Navigation, and Control Conference and Exhibit*. 2004, pp. 16–19.

[59] William J. Pisano and Dale A. Lawrence. “Control Limitations of Small Unmanned Aerial Vehicles in Turbulent Environments”. In: *Proceedings of the AIAA Guidance, Navigation, and Control Conference*. 2009.

[60] T.N. Pornsin-sirirak et al. “MEMs Wing Technology for a Battery Powered Ornithopter”. In: *IEEE* (2000), pp. 799–804.

[61] T.N. Pornsin-sirirak et al. *Microbat: A Palm-Sized Electrically Powered Ornithopter*. Tech. rep. Aerovironment, 2013.

[62] Paul I.E. Pounds, Daniel R. Bersak, and Aron M. Dollar. “Grasping From the Air: Hovering Capture and Load Stability”. In: *Proceedings of the IEEE Conference on Robotics and Automation*. 2011.

[63] Raymond W. Prouty. *Helicopter Performance, Stability and Control*. Krieger Publishing Company, 2005.

[64] R. Randolph. *R-C Airplane Building Techniques*. R/C Encyclopedia Series. Air Age Pub., 1991. ISBN: 9780911295139.

[65] D.P. Raymer, American Institute of Aeronautics, and Astronautics. *Aircraft design: a conceptual approach*. Educ Series. American Institute of Aeronautics and Astronautics, 1989. ISBN: 9780930403515.

[66] S.P. Sane. “The aerodynamics of insect flight”. In: *Journal of Experimental Biology* (2003), pp. 4191–4208.

[67] S.P. Sane and M.H. Dickinson. “The control of flight force by a flapping wing: lift and drag production”. In: *Journal of Experimental Biology* (2001), pp. 2607–2626.

[68] D Scaramuzza et al. “Vision-controlled micro flying robots: from system design to autonomous navigation and mapping in GPS-denied environments”. In: *IEEE Robotics & Automation Magazine* (2014), pp. 1–10.

[69] Wei Shyy et al. *An Introduction to Flapping Wing Aerodynamics*. Vol. 37. Cambridge University Press, 2013.

[70] Henkk Tennekes. *The Simple Science of Flight: From Insects to Jumbo Jets*. The MIT Press, 2009.

[71] Mark B. Tischler and Robert K. Remple. *Aircraft and Rotorcraft System Identification: Engineering Methods with Flight-Test Examples*. American Institute of Aeronautics and Astronautics, 2006.

[72] Teodor Tomic et al. "Toward a Fully Autonomous UAV: Research Platform for Indoor and Outdoor Urban Search and Rescue". In: *IEEE Robotics & Automation Magazine* 19.3 (Sept. 2012), pp. 46–56.

[73] Evan R. Ulrich, J. Sean Humbert, and Darryll J. Pines. "Pitch and Heave Control of Robotic Samara Micro Air Vehicles". In: *Journal of Aircraft* 47 (2010), pp. 1290–1299.

[74] D.R. Warrick, B.W. Tobalske, and D.R. Powers. "Lift production in the hovering hummingbird". In: *Proceedings of the Royal Society Biological Sciences* (2009), pp. 3747–3752.

[75] Stephan Weiss. "Vision based navigation for micro helicopters". PhD thesis. ETH Zurich, 2012.

[76] Jan Willmann et al. "Aerial robotic construction towards a new field of architectural research". In: *International journal of architectural computing* 10.3 (2012), pp. 439–460.

[77] J. Young et al. "Details of Insect Wing Design and Deformation Enhance Aerodynamic Function and Flight Efficiency". In: *Science* (2009), pp. 1549–1552.

[78] Chul Yong Yun et al. "A New VTOL UAV Cyclocopter with Cycloidal Blades System". In: *Proceedings of the 60th AHS Annual Forum of the American Helicopter Society*. 2004.

[79] Luca Zaccarian. "DC motors: dynamic model and control techniques". In: *Lecture Notes., Roma, Italy* (2012).

[80] L. Zhao et al. "Aerodynamic effects of flexibility in flapping wings". In: *Journal of the Royal Society Interface* (2010), pp. 485–497.

[81] LIN Zongjian. "UAV for mappinglow altitude photogrammetric survey". In: *International Archives of Photogrammetry and Remote Sensing, Beijing, China* (2008).